

## CHAPTER 82

# Irregular Waves on a Current

H.-H. Prüser and W. Zielke <sup>1</sup>

### 1 Introduction

In coastal areas interacting currents and waves are quite frequent. The currents are generated by the tides or the discharge of a river; the waves are irregular short crested, generated by the wind. A suitable numerical wave model for this situation is presented in this paper. It is based on the Boussinesq-Wave-Equations (BWE) which were extended to simulate the influence of a current on a wave as well as the effects of nonlinear wave-wave interaction in a propagating wave spectrum.

An analytical approach to describe wave-current interaction was given by Longuet-Higgins/Steward (1960) [3]. They investigated linear small amplitude waves in a moving medium and introduced the concept of radiation stress to determine the change of wavelength and wave amplitude as a function of the current and the direction of wave propagation. Their fundamental work was the basis for the development of various numerical models, which were reviewed recently by Jonsson (1989) [2]. Most of these models are restricted to linear (small amplitude) wave theory.

The wave climate in shallow water is generated by the influence of bottom topography as well as by nonlinear wave-wave interaction in a propagating wave spectrum, which cannot be described by linear wave theory. Instead, such weakly nonlinear waves are frequently modeled using the BWE. The development of models based on these equations first began in the late 70's. Since then, a number of studies have been carried out to verify their capabilities. It has been shown that they are able to simulate accurately combined refraction, diffraction, reflection and shoaling (see for example Madsen/Warren (1984)[4] as well as the nonlinear wave-wave interaction in a wave spectrum propagating over an uneven bed (see for example Prüser/Schaper/Zielke (1986)[7]). Boussinesq wave models have now become a practical tool for engineering applications.

In this paper, a numerical model based on an extended form of the BWE which takes into account the influence of an ambient current on waves is used to investigate irregular waves propagating and refracting on an ambient current. After presenting the equations, a comparison based upon linear (small amplitude) wave theory is conducted to illustrate the range of application. The numerical model was used to simulate irregular waves with a current in a flume and in a basin. The results were in good agreement with the solution of Longuet-Higgins/Steward.

---

<sup>1</sup>Institute of Fluid Mechanics, University of Hannover, Appelstr. 9A, 3000 Hannover, F.R.G.

## 2 The mathematical model

### 2.1 The Extended Boussinesq-Wave-Equations

Nonlinear wave behaviour in shallow water and in intermediate depth can be simulated using the BWE. These equations have been extended in order to include the effect of wave-current interaction, which is often necessary in coastal areas. *Mathematically, the general case of waves propagating through a current field over an arbitrary bottom topography is a complex initial boundary value problem. However, since the length and time scales of the wave motion are usually much smaller than those of the current, it is possible to solve the current field and the wave field in two separate steps*<sup>2</sup>. Consequently, for the derivation of the extended BWE, it is assumed that the current field is known from numerical simulations or measurements. A step by step description is given by Prüser (1991)[6]. The extended BWE used in this paper and the equation of continuity are as follows (the index '0' refers to the ambient current and '\*' to the combined flow of waves and currents. Variables without indices refer to waves only) :

$$\begin{aligned}
 u_{,t} + u^*u_{,x} + v^*u_{,y} + g\zeta_{,x} &= -\frac{D^2}{6}(u_{,xxt} + v_{,xyt}) + \frac{D}{2}((u_{,t}D)_{,xx} + (v_{,t}D)_{,xy}) \\
 &\quad + u_0\frac{D^2}{3}(u_{,xxx} + v_{,xxy}) + v_0\frac{D^2}{3}(u_{,xxy} + v_{,yyy}) \quad (1)
 \end{aligned}$$

$$\begin{aligned}
 v_{,t} + u^*v_{,x} + v^*v_{,y} + g\zeta_{,y} &= -\frac{D^2}{6}(u_{,xyt} + v_{,yyt}) + \frac{D}{2}((u_{,t}D)_{,xy} + (v_{,t}D)_{,yy}) \\
 &\quad + u_0\frac{D^2}{3}(u_{,xxy} + v_{,xyy}) + v_0\frac{D^2}{3}(u_{,xyy} + v_{,yyy}) \quad (2)
 \end{aligned}$$

$$(D + \eta)_{,t} + (u^*(D + \eta))_{,x} + (v^*(D + \eta))_{,y} = 0 \quad (3)$$

with:  $u^* = u + u_0 \quad v^* = v + v_0$

The fluid velocities  $u^*$ ,  $v^*$  are comprised of the ambient current field  $u_0$ ,  $v_0$  and the wave flow field  $u$ ,  $v$ . The current appears in the convective terms of the left hand side of the equations and also produces additional third order terms. The numerical BOUSSINESQ-WAVE-MODEL (BOWAM) which was available for the solution employs a formulation involving fluxes and surface elevations [8] [9]. Therefore, it was necessary to transform the equations by substituting  $h = D + \zeta$ ,  $p = uh$  and  $q = vh$ . The equations were solved by an implicit third order corrected finite difference method using two time levels and central differences.

### 2.2 Range of application, harmonic waves

The range of application depends on the wavelength to water depth ratio  $L/D$ . Shallow water is defined if the wavelength is larger than 20 times the water depth whilst deep water is defined if the wavelength is smaller than twice the

---

<sup>2</sup>cited from Jonsson[2]

wavelength; the region between these limits is referred to as intermediate depth. The BWE are limited to shallow water with an extension to include intermediate depth. In a nonlinear study with periodic waves, McCowan (1987)[5] has shown that the equations are valid provided the wavelength is at least 6 times the water depth. In this paper, the range of application for the extended BWE will be checked by a comparison with linear (small amplitude) wave theory. In a first step, the dispersion relations will be investigated. These results are necessary to subsequently verify the extended BWE using analytical solutions of wave-current interactions.

The wave profile is given by a harmonic function with amplitude  $a$ , wave number  $k = 2\pi/L$  and frequency  $\omega = 2\pi/T$ .

$$\eta(x, t) = a \sin(\omega t - kx) \tag{4}$$

For simplicity, the investigation is limited to the one-dimensional case with constant water depth. The BWE and the equation of continuity reduce to:

$$u_{,t} + (u_0 + u)u_{,x} + g\eta_{,x} - \frac{1}{3}D^2u_{,xxt} - \frac{1}{3}D^2u_0u_{,xxx} = 0 \tag{5}$$

$$\eta_{,t} + u_0\eta_{,x} + Du_{,x} = 0 \tag{6}$$

The velocity  $u$  can be eliminated by differentiating (5) with respect to  $x$  and substituting (6) in (5). Finally, nonlinear terms of order  $O(a^2)$  are neglected.

$$-\eta_{,tt} + (gD - u_0^2)\eta_{,xx} - 2u_0\eta_{,xt} + \frac{D^2}{3}(\eta_{,xxtt} + 2u_0\eta_{,xxxxt} + u_0^2\eta_{,xxxxx}) = 0$$

Inserting the wave profile (4) into the above equation gives Equ. (7). Nontrivial solutions for the frequency  $\omega$  (8) are obtained if the first parenthesis is set to zero.

$$\left(\omega^2 - 2ku_0\omega + k^2u_0^2 - \frac{k^2gD}{1 + \frac{1}{3}D^2k^2}\right) a \sin(\omega t - kx) = 0 \tag{7}$$

$$\omega_{1,2} = ku_0 \pm \sqrt{\frac{k^2gD}{1 + \frac{1}{3}k^2D^2}} \tag{8}$$

The sign in front of the square root is chosen according to whether the wave is propagating in the direction of the current  $u_0$  or in the opposite direction. The differentiation of  $\omega$  with respect to the wave number  $k$  gives the group velocity:

$$c_g = \frac{\partial\omega}{\partial k} = \frac{1}{2}c^B(1 + G^B) + u_0$$

$$\text{mit: } G^B = \frac{1 - \frac{1}{3}k^2D^2}{1 + \frac{1}{3}k^2D^2} \tag{9}$$

Table 1 summarizes the analytical formulae for the dispersion relation of the linear theory and of the Boussinesq theory in the case of small amplitude waves.

and Steward. The wavelength in the presence of a current is given by an implicit function of the corresponding wave in still water (frequency  $\omega$ ; phase velocity  $c$ ) and the current  $u_0$ :

$$L^c = 2\pi k^c \quad \text{with} \quad (\omega - k^c u_0)^2 = k^c \omega c \quad (10)$$

The change of wave amplitudes depends on the manner in which the ambient current is generated. Longuet-Higgins/Steward investigated two different situations, which were defined as *upwelling from below* and *inflow from the sides*. These definitions will be explained in the Chap. 3.1. In the case of *upwelling from below*, an adequate formula describing the situation with a current ( $a^c, L^c, G^c$ ) and the situation in still water ( $a, L, G$ ) is given by Brevik/Aas (1980)[1]. The change of amplitudes tends towards infinity as the Froude number tends towards  $Fr \rightarrow -0.5$ :

$$\frac{a^c}{a} = \sqrt{\frac{1 + G}{\left(\frac{L^c}{L} - \frac{u_0}{c}\right)(1 + G^c) + \frac{2u_0}{c}\left(1 - \frac{L}{L^c} \frac{u_0}{c}\right)}} \quad (11)$$

The parameters  $G, G^c, L^c$  and  $c$  can be substituted by the dispersion relations summarized in Table 1. Fig. 2 shows the change of wavelength  $L^c/L$  and Fig. 3 shows the change of wave amplitude  $a^c/a$  as a function of the Froude number  $Fr = u_0/\sqrt{gD}$  for three different wavelengths ( $L/D = 20, 10, 6$ ). The solid lines indicate the results obtained from the formulae (10) and (11) using linear theory whilst the dashed line indicate the results from Boussinesq theory. A negative Froude number indicates that the current and waves are propagating in opposite directions. The formulae are evaluated for Froude numbers  $-0.3 < Fr < 0.5$ . For most coastal engineering purposes, however, Froude numbers lie in the range of  $-0.2 < Fr < 0.2$ . With regard to the change of wavelength  $L^c/L$ , the following can be stated:

- The wavelength increases if the direction of wave propagation is the same as that of the current ( $Fr > 0$ ) and decreases in the case of opposite directions. This effect is more pronounced in deeper water.
- The Boussinesq approximation is very good for the complete range of Froude numbers in Fig. (2) provided the wavelength is larger than 10 times the water depth.

With regard to the change of wave amplitude  $a^c/a$ , the following can be stated:

- The wave amplitude increases if the direction of wave propagation and that of the current are different ( $Fr < 0$ ) and decreases when the directions are the same.
- The influence of the relative wavelength  $L/D$  on the change of amplitudes is very slight for Froude numbers greater than zero, but significant for Froude numbers less than zero.

	linear theory	Boussinesq theory
phase velocity $c^c = u_0 + c$	$c^L = \sqrt{gD} \sqrt{\frac{1}{kD} \tanh kD}$	$c^B = \sqrt{gD} \sqrt{\frac{1}{1 + \frac{1}{3} k^2 D^2}}$
group velocity $c_g^c = u_0 + \frac{1}{2} c(1 + G)$	$G^L = \frac{2kD}{\sinh 2kD}$	$G^B = \frac{1 - \frac{1}{3} k^2 D^2}{1 + \frac{1}{3} k^2 D^2}$

Table 1: Dispersion relation in linear and Boussinesq theory

The superscript *c* indicates currents, *L* indicates Linear theory, and *B* indicates Boussinesq theory. The comparison indicates a high degree of similarity between linear and Boussinesq theory. If an ambient current is present, then the phase velocity *c<sup>c</sup>* and the group velocity *c<sub>g</sub><sup>c</sup>* are superposed on the current *u<sub>0</sub>* and the corresponding velocity in still water. For shallow water conditions (*kD* → 0), linear and Boussinesq theory are identical. In deeper water however, the solution obtained by Boussinesq theory is an approximation to linear theory.

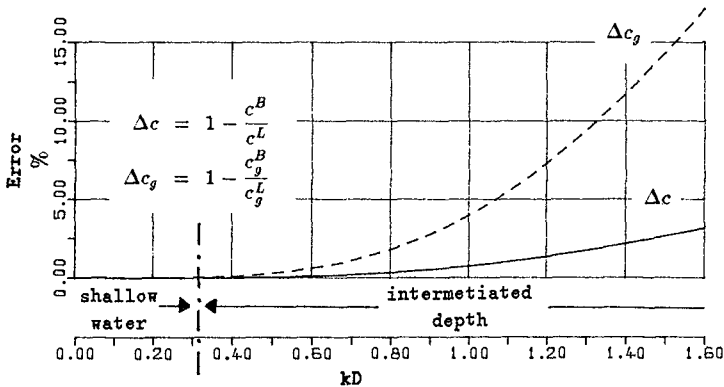


Figure 1: Dispersion relation in linear and Boussinesq theory as a function of the parameter *kD*

Fig. 1 displays the relative errors of the phase velocity  $\Delta c$  (solid line) and the group velocity  $\Delta c_g$  (dashed line) as a function of the parameter *kD*. As expected, an excellent agreement is found between linear and Boussinesq theory for shallow water conditions (*L/D* > 20, *kD* < 0.3). Moving into deeper water (*kD* > 0.3), Boussinesq approximation for the phase velocity is much better than for the group velocity. A priori we will allow errors in phase and group velocity less than 5%, which gives a limit for the range of application of *kD* < 1.0 (see Fig. 1). This is in agreement with McCowan who indicated that the wavelength should be larger than 6 times the water depth.

The change of wavelength and wave amplitude due to the ambient current can be determined by analytical solutions based on the work of Longuet-Higgins

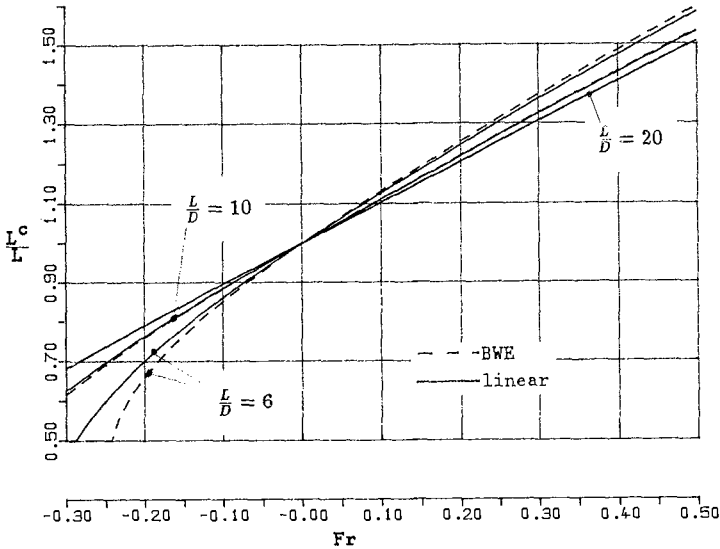


Figure 2: Change of wavelength due to an ambient current. Comparison with the corresponding wavelength in still water.

- For negative Froude numbers, the wavelength must be larger than 10 times the water depth.

In conclusion: Within limits of linear wave theory, extended BWE are valid for simulating the interaction of an ambient current on waves if the corresponding wavelength in still water is larger than 10 times the water depth and the Froude number is in the range of  $-0.2 < Fr < 0.2$ . If the corresponding wavelength in still water is smaller than 10 times the water depth and larger than 6 times the water depth, the extended BWE are applicable only if wave and current are in the same direction. If the waves are even shorter than 6 times the water depth, they are outside the range of Boussinesq theory, independent upon the current direction.

### 2.3 Range of application, irregular waves

The investigation on the basis of the dispersion relation, as presented in Chap. 2.2, is necessarily limited to harmonic waves with particular frequencies and wavelengths. The natural sea state, however, contains various interacting wave components. There is a need to define, which type of spectra and which frequency range can be modeled properly with BWE. Due to the nonlinear character of the waves there is no analytical theory available to define the range of validity. On the basis of experience, which has been obtained in a quite number of BOWAM-Simulations the following statements can nevertheless be made:

In irregular wave trains short waves are often related to longer waves. One ex-

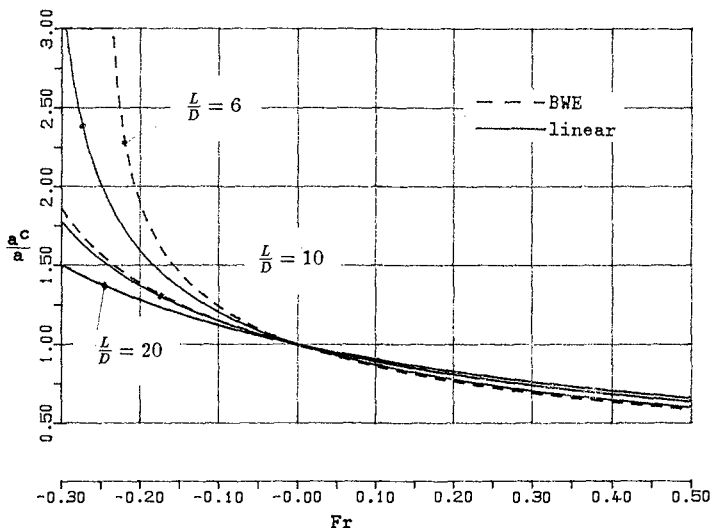


Figure 3: Change of wave amplitude due to an ambient current. Comparison with the corresponding wave amplitude in still water.

ample is the behaviour of wave groups. Hydraulic measurements and the theory of biharmonic waves have shown, that bounded-long waves as well as bounded-short waves are generated. Another example is the propagation of a wave spectrum from deeper to shallower water. A transformation of energy towards higher harmonics can be observed. The centre-row of Fig. 6 demonstrates this quite clearly. In both cases, the high frequency components (short waves) which are created in the transformation may be outside of the range of validity of BWE as defined in Chap. 2.2. However, they can be properly modeled with BWE as long as the corresponding long waves are in the range of validity.

### 3 Waves on a current in a flume

#### 3.1 Generation of the current

The current can be generated by pumping water into the flume through an inlet (or outlet) located at the bottom or in the walls. In the following it will be assumed that this volume flux is constant in time. The current velocity  $u_0$  can be changed, however, by increasing or decreasing the cross-section of the flume. The change of wave amplitudes caused by the ambient current depends on *how* the current is generated. In the case of an upwelling of water from below (inlet at the bottom, varying water depth), it is larger than in case of inflow from the sides (inlet in the wall, narrowing of the width of the flume). Both cases will be investigated numerically. In Fig. 4, the corresponding analytical solutions for shallow water conditions and constant water depth are shown. A negative current with a Froude number of  $Fr = -0.2$  shows an increase of the amplitudes of about

10% for the case of *inflow from the sides* and of about 25% for the case of *upwelling from below*. The change of wavelength is the same in both cases.

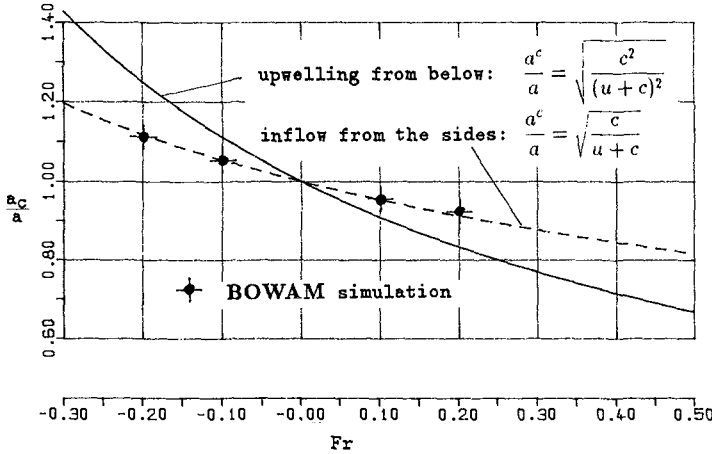


Figure 4: Change of amplitudes in shallow water. Comparison of the situations *upwelling from below*, *inflow from the sides* and BOWAM-Simulation.

### 3.2 Inflow from the sides

The behaviour of a wave spectrum propagating in a wave flume with constant water depth was investigated using the BWE. The upper part of Fig. 5 displays the experimental set-up: A numerical wave flume with a wave maker on the left hand side and three velocity/water elevation gauges A, B, C is shown. The water depth ( $D = 0.5m$ ) as well as the width of the flume are constant. A number of inlets in the walls enable an ambient current to be generated between the gauges A and B by an *inflow from the sides*. The current  $u_0$  is assumed to be zero at gauge A, increasing linearly to gauge B and remaining constant between gauges B, C.

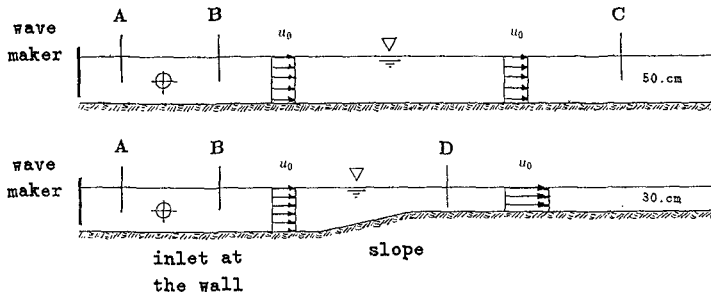


Figure 5: Experimental set-up: Waves with an ambient current in a wave flume

Pierson–Moskowitz spectra are introduced into the flume by the wave maker. The simulated time series of the surface elevation  $\eta$  are recorded at the gauges. These were transformed by FFT into the frequency domain to investigate the change of the spectral shape along the flume. Fig. 6 displays the calculated wave spectra at the gauges A, B, C for different ambient currents. The total amount of energy is given by the spectral moment of zero order  $m_0$ . Assuming a *Rayleigh* distribution, the significant wave height can be calculated from:

$$H_s = H_{m0} = 4\sqrt{m_0} \quad (12)$$

The spectra along the centre-row of Fig. 6 are the results of a simulation in still water ( $Fr = 0.$ ). The significant wave height  $m_0$  is the same for all gauges. For deep water conditions the incoming Pierson–Moskowitz spectrum is stable. In Fig. 6 the wavelength corresponding to the peak period of the spectrum ( $T_p = 4.5s$ ) is about 20 times the water depth, which indicates shallow water conditions. Therefore, due to nonlinear wave–wave interaction in shallow water, the spectral shape changes considerably. Higher harmonics and low frequency components bounded to wave groups have been generated. This is visible in the spectral shape. A double peaked spectrum and lower frequency components not included in the input spectrum appear at gauge C. The numerical simulation without a current has been verified very successfully by hydraulic measurements for a number of different wave spectra (Prüser/Schaper/Zielke [7]). It can be used to estimate and compare the influence of the ambient current.

The first and third row of Fig. 6 display the influence of wave–current interactions. The Froude number of the ambient current was  $Fr \pm 0.1$ , i.e. the investigation deals with waves propagating in the direction of the current as well as in the opposite direction. The recorded time series at gauge A is equal in both cases because the current is zero at this location. The wave spectrum at gauge A is given in the centre-row. The influence of the ambient current on the wave spectrum can be separated into two phenomena:

The first one concerns the change of significant wave heights  $H_s$  between gauges A and B. If waves and currents are propagating in the same direction, the amplitudes i.e. the energy corresponding to the individual frequency components have decreased. The spectral moment of first order changes from  $m_0 = 8.6 \cdot 10^{-5}$  to  $7.8 \cdot 10^{-5}$  (the reverse effect occurs if waves and current are propagating in opposite directions  $m_0 = 8.6 \cdot 10^{-5}$  to  $9.6 \cdot 10^{-5}$ ). This gives significant wave height ratios of  $H_s^c/H_s = 0.95$  and  $H_s^c/H_s = 1.06$ , respectively). Further investigations show, that these ratios are nearly independent upon the incoming wave height  $H_s$ , but they do depend on the peak–period of the spectrum. This is in agreement with Fig. 11. For shallow water conditions and a current, generated by an *inflow from the sides*, the results of BOWAM are very close to the analytical solution, as shown in in Fig. 4. The second phenomenon concerns nonlinear wave–wave and wave–current interactions. These can be obtained by comparing the wave spectra at the gauges B and C for the three test conditions displayed in Fig. 6. Double peaked spectra are generated and the total amount of energy

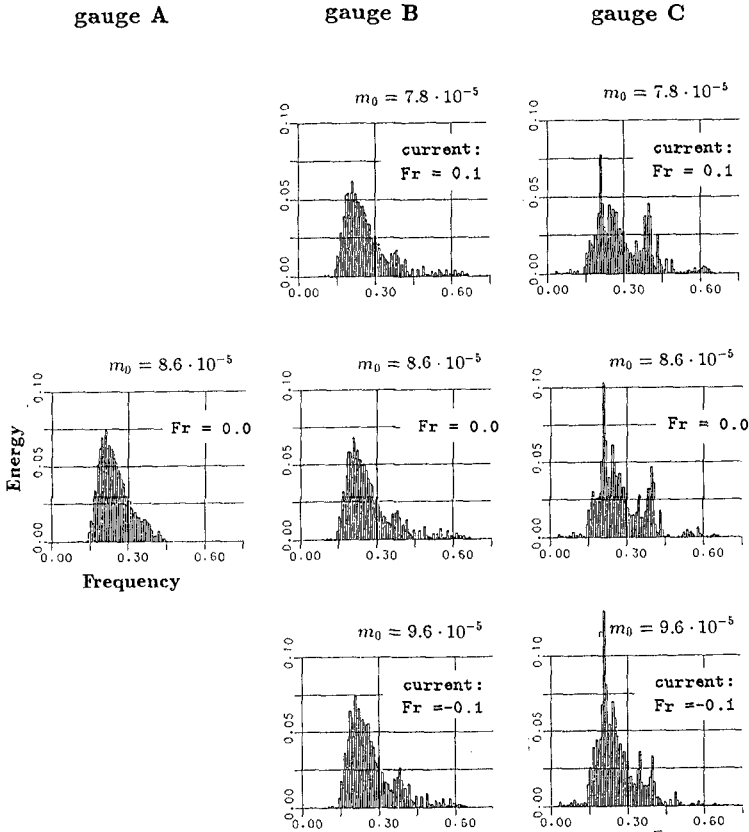


Figure 6: Wave-current interaction in the frequency domain

is constant for each test. However, the behaviour of the peaks at a frequency of  $\approx 0.2Hz$  and  $\approx 0.4Hz$  is different. The first peak decreases if waves and current are propagating in the same direction and increases otherwise. This is again in agreement with Fig. 4. The behaviour of the second peak is almost the reverse of the latter. It remains constant or increases if waves and current are in the same direction and decreases otherwise. This cannot be explained by the theory of Longuet-Higgins/Steward. Although the significant wave height of the spectrum is relatively small compared to the water depth ( $H_s \approx 4.cm$   $D = 50.cm$ ), the nonlinear wave-wave interaction between the individual frequency components dominates the influence of wave-current interaction. Contrary to the first phenomenon there is a significant dependency on the incoming wave height, indicating the necessity of nonlinear numerical simulations.

### 3.2 Upwelling from below

The bottom picture of Fig. 5 displays the experimental set-up. This is almost the top picture, except that a slope is present between gauges **B** and **D** and the water depth reduces from 50.cm to 30.cm. Consequently, the wave transformation is even more complicated. Due to the different cross-sections, the ambient current is larger at gauge **D** than at gauge **A**. The change of the current takes place above the slope by an upwelling of water from below. In addition to this, the propagating wave spectrum shoals over the slope.

Assuming a linear, monochromatic wave, the change of its amplitude between gauges **B** and **D** can be calculated using the formula<sup>3</sup>

$$\frac{a^D}{a^B} = \sqrt{\frac{(u_{0,B} + \frac{1}{2}c_B(1 + G_B)L_B)c_D}{(u_{0,D} + \frac{1}{2}c_D(1 + G_D)L_D)c_B}} \quad (13)$$

If the ambient current is zero at both gauges ( $u_{0,B} = u_{0,D} = 0$ ), then (13) gives the shoaling coefficient. If  $u_{0,B} = 0$  and the water depths are equal at both gauges, then (13) is identical to Equ. (11). It is important to notice that the change of amplitudes results from a combination of wave-current interaction and shoaling.

As indicated in Chap. 3.2, the significant wave height of the spectrum  $H_s$  is affected by an ambient current as predicted by the analytical solution of Longuet-Higgins/Steward. This chapter is to investigate further changes in a combined current-shoaling situation. A suitable numerical model has to take into account that waves are transformed by an upwelling of water from below. In other words, it has to take into account a vertical component of the fluid velocity above the slope. Although the variables of the extended BWE are the depth-averaged horizontal velocities  $u, v$ , a vertical velocity  $w$  varying linearly from the bottom to the surface is assumed during the derivation. This enables the equations to simulate the wave behaviour above the slope which is influenced by water *upwelling from below*.

Several numerical simulations have been carried out using a Pierson-Moskowitz spectrum with different peak periods  $T_p$  and different significant wave heights  $H_s$ . Also, a comparison is made using Equ. (13), involving a monochromatic wave with a period equal to the peak period of the spectrum. Table 2 summarizes the results for a spectrum with  $T_p = 4.5s$  and different current conditions: Column *BOWAM* displays the results of the numerical model whereas column *combined* shows the results of the analytical solution (13). It is common practice in simple linear wave modelling to approximate combined effects as a superposition of individual effects. For comparison, column  $k_s$  and column  $k_u$  are the results of separate shoaling and separate wave-current interaction, respectively. Column  $k_{s,u} = k_s k_u$  displays the results of the linear superposition.

It can be stated that the results of BOWAM are in very good agreement with the analytical solution. The linear superposition of separate shoaling and

<sup>3</sup>This formula has been developed based on the concept of the *conservation of wave action*. For details, see Jonsson [2] and Prüser[6].

gauge B		gauge D		$H_{s,D}/H_{s,B}$				
$u_0$	Depth	$u_0$	Depth	BOWAM	combined	$k_s$	$k_u$	$k_{s,u}$
0.100	0.50	0.167	0.30	1.068	1.070	1.125	0.970	1.091
-.100	0.50	-.167	0.30	1.200	1.192	1.125	1.036	1.166
0.150	0.50	0.250	0.30	1.039	1.048	1.125	0.957	1.077
-.150	0.50	-.250	0.30	1.241	1.232	1.125	1.057	1.189

Table 2: Combined modelling of waves on a current and shoaling

separate wave current interaction is a relatively good approximation regarding wave heights. It should not be used, however, if one is interested in locating a breaker zone, which depends on the ratio of wave height to water depth; irregular wave trains will produce a time-varying breaker zone. This has to be simulated in nonlinear wave models.

#### 4 Waves on a current in a basin

The corresponding two-dimensional extension of the test described in Chap. 3.2 will be investigated here. In a wave basin of constant water depth ( $D = 50\text{ cm}$ ), a Pierson-Moskowitz spectrum ( $T_p = 4.5s$ ,  $H_s \approx 4\text{ cm}$ ) is generated by the wave maker and propagates from left to right. An ambient current with a Froude number of  $Fr = \pm 0.1$  is assumed in a part of the computational domain.

The situations: a) waves and current propagating in the same direction; b) no current; c) waves and current propagating in opposite directions are displayed from top to bottom in Fig. 7.

The wave crests at a specific time step are given on the left hand side. The darker the wave crests, the higher is the surface elevation. A numerical, directional wave gauge is placed in the basin to obtain the spectral shape of the spectrum and the distribution of the mean direction as a function of the frequency. In the case of still water, the transformation is the same as displayed along the centre-row of Fig. 6. The mean direction is constant at  $\Theta = 90^\circ$  and the spectral moment  $m_0 = 8.6 \cdot 10^{-5}$ .

In the presence of a current, the wave fronts change their direction. In the case of waves and current in the same direction, the waves are refracted with an average angle of  $\Delta\Theta = 10^\circ$  at the gauge (For waves and current in opposite directions the angle of refraction is  $\Delta\Theta = 12^\circ$ ). The quantity  $\Delta\Theta$  depends on current and frequency. High components are refracted more than low components.

At the transition between still water and current, the crests are drawn apart. This produces a two-dimensional effect in which wave energy propagates along the crests. A decrease or increase of the spectral moment  $m_0$  was recorded. This depends on the current condition and on the position in the computational domain. The change can be very much higher than predicted in the one-dimensional test (Chap. 3.2). Fig. 7 shows that in the case of waves and current in the same direction, the spectrum remains single-peaked ( $m_0 = 5.1 \cdot 10^{-5}$ ) at the chosen

gauge. A double-peaked spectrum ( $m_0 = 11.5 \cdot 10^{-5}$ ) is generated if waves and current are in opposite directions.

The numerical model was also used to simulate arbitrary angles between the current and the wave direction. Although, the results were very promising, they are not presented here because corresponding hydraulic measurements were not available for verification purposes.

## 5 Conclusions

A numerical model based on the extended Boussinesq-Wave-Equations (BWE) was applied to simulate irregular waves with an ambient current. The current alters wave height, wavelength and the direction of wave propagation. The equations may be used to simulate the generation or the change of a current by an *inflow from the sides* as well as by an *upwelling from below*.

The range of validity has been checked, comparing Boussinesq theory with linear wave theory. Regarding harmonic waves, the BWE are valid provided the wave length is at least 10 times the water depth and the Froude number of the current is smaller than  $\pm 0.2$ . Regarding irregular waves, even shorter waves of a spectrum can be simulated as long as they are related to long waves (bounded-short waves, the generation of higher harmonics).

The change of the significant wave height of a Pierson-Moskowitz spectrum can be predicted by the theory of Longuet-Higgins/Stewart using a monochromatic wave with the peak period of the spectrum. The change depends on the period of the wave, the strength of the current and the water depth. The wave amplitude itself has a minor effect. The results of the numerical model are in very good agreement with the theory. The numerical model also simulates the development of the spectral shape.

## References

- [1] I. Brevik and B. Aas. Flume experiments on waves and currents. *Coastal engineering*, 3, 1980.
- [2] I.G. Jonsson. Wave-current interactions. *Report No. S 49*, 1989. The Danish Center for Applied Mathematics and Mechanics. Institute of Hydrodynamics and Hydraulic Engineering.
- [3] M.S. Longuet-Higgins and R.W. Stewart. The changes in amplitude of short gravity waves on steady non-uniform currents. *Journal of fluid mechanics*, 10, 1961.
- [4] P.A. Madsen and I.R. Warren. Performance of a numerical short-wave model. *Coastal Engineering*, 8, 1990.
- [5] A.D. McCowan. The range of application of Boussinesq type numerical short wave models. In *IAHR-Congress*, 1987. Lausanne.

- [6] H.-H. Prüser. Zur Interaktion von Wellen und Strömung im flachen Wasser. *Report No. 30*, Institut für Strömungsmechanik und elektronisches Rechnen im Bauwesen, Universität Hannover, 1991.
- [7] H.-H. Prüser, H. Schaper, and W. Zielke. Irregular wave transformation in a Boussinesq wave model. In *20nd International Conference on Coastal Engineering*, 1986. Taipei.
- [8] H. Schaper. Ein Beitrag zur numerischen Berechnung von nichtlinearen kurzen Flachwasserwellen mit verbesserten Differenzenverfahren. *Report No. 21*, Institut für Strömungsmechanik und elektronisches Rechnen im Bauwesen, Universität Hannover, 1985.
- [9] H. Schaper and W. Zielke. A numerical solution of the Boussinesq type wave equations. In *19nd International Conference on Coastal Engineering*, 1984. Houston.

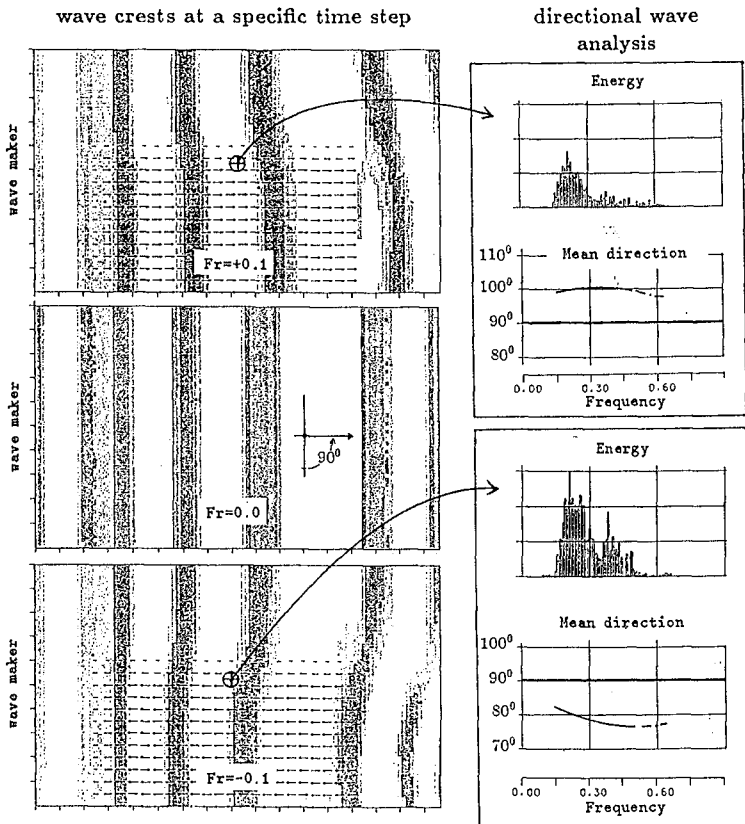


Figure 7: Waves with a current in a basin